Dynamic Rolling-Walk Motion by the Limb Mechanism Robot ASTERISK

Chayooth Theeravithayangkura *, **Tomohito Takubo**, **Kenichi Ohara**, **Yasushi Mae** and **Tatsuo Arai**

Division of System Innovations, Graduate School of Engineering Science, Osaka University, 1-3 Machikaneyama, Toyonaka, Osaka 560-8531, Japan

Received 6 November 2009; accepted 16 February 2010

Abstract

New dynamic rolling-walk motion for a multi-legged robot with error compensation is proposed. The motion is realized by using the isotropic leg arrangement and the dynamic center of mass control inspired by bipedal robots. By using the preview control of the zero moment point (ZMP) with a cart-table model based on the bipedal robot's technique, the robot's center of mass trajectory is planned for the dynamic motion. The resolved momentum control for manipulating the multi-links robot as a single mass model is also implemented in the system to maintain the stability of the robot. In the new dynamic rolling-walk motion, the robot switches between the two-leg supporting phase and three-leg supporting phase to achieve dynamic motion with the preview control of the ZMP and resolved momentum control as dynamic motion controllers. The authors analyzed the motion and confirmed the feasibility in the Open Dynamics Engine before testing the motion with an actual robot. Due to the difficulties of controlling the ZMP during the two-leg supporting phase, the authors implemented error compensation by using a gyro sensor and compared the results.

Keywords

Dynamics, preview control, resolved momentum control, multi-legged robot, mobile robot

1. Introduction

Over recent decades, many researchers have focused on mobile robots as their broad applications are very promising. Most of the research has been on the duplication of human or animal movements. For robot mobility, surrounding environment recognition, human recognition and human–robot communication research are also very interesting. It is important for a robot to have those abilities so that it may be introduced into real-world applications to aid or replace humans in dangerous tasks.

As dynamic motion and mechanics of robot movement are generally inspired by animals, many researchers have tried to implement animal characteristic in their robots to achieve efficient and attractive mobility. Unique mobile robots are proposed based on the mechanic and dynamic originality of the researchers.

Morazzani *et al.* [1] proposed a new tripedal mobile robot named STriDER and its gait planning strategy. The locomotion style is novel. The dynamics and trajectory planning are kinematically derived by their unique idea. The walking motion is self-excited by the proper preliminary motion and its motion provides efficient energy saving without sophisticated control methods. Likewise, Schroer *et al.* [2] presented a new locomotion style by using a Wheg, which is a spoke-like leg driven by a single DC motor; it provides feet-like foot stamps and moves by motor rotation. The Wheg is implemented in the same way as a six-wheeled vehicle and their setting angles are arranged to keep a tripod-like foothold by synchronous rotation of Whegs. The locomotion technique is inspired by the cockroach, but the implementation is based on the mechanical uniqueness of the researchers. Similarly, Moore *et al.* [3] also used Whegs as legs on their hexapod robot named RHex. It consists of six Whegs implemented with the compliance structure. They presented experimental results on very rough terrain and a particular flight of stairs to show the ability to traverse. Their unique and high mobility is achieved by using rotating legs. The spoke-like rotational leg model was proposed as a bipedal model of passive walking on an inclined plane by McGeer *et al.* [4]. As passive walking has high robustness and high efficiency, the model that could achieve these abilities is very promising for future studies. Furthermore, Sastra *et al.* [5] introduced dynamic rolling for a modular loop robot called Connector Kinetic roBot (CKBot). They designed a dynamic rolling gait that provides a good distance with reasonable speed. They also made a comparison between the dynamic and kinetic rolling motion. Such dynamic motion-related research gave us the inspiration to start the dynamic rolling-walk on our limb mechanism robot ASTERISK.

A problem arose when the authors were considering what kind of dynamic motion should be designed. The authors chose to consider the situation where the robot cannot move further by using the motion it already realized. Therefore, in this experiment, the authors would like to design a new dynamic motion so that the robot can go through narrow spaces where no kinetic movement can.

2. Limb Mechanism Robot ASTERISK

The limb mechanism robot ASTERISK, a working mobile robot, consists of multiple limbs that can be used as both legs for locomotion and arms for manipulation depending on the present situation.

ASTERISK has six limbs attached to the body radially at even intervals of 60°. This arrangement gives the robot homogeneous mobility and manipulation ability in all horizontal directions. Each of its limbs consists of three rotational joints; thus the robot has 18 d.o.f. (Fig. 1). The authors numbered each leg from 10 to 60 and

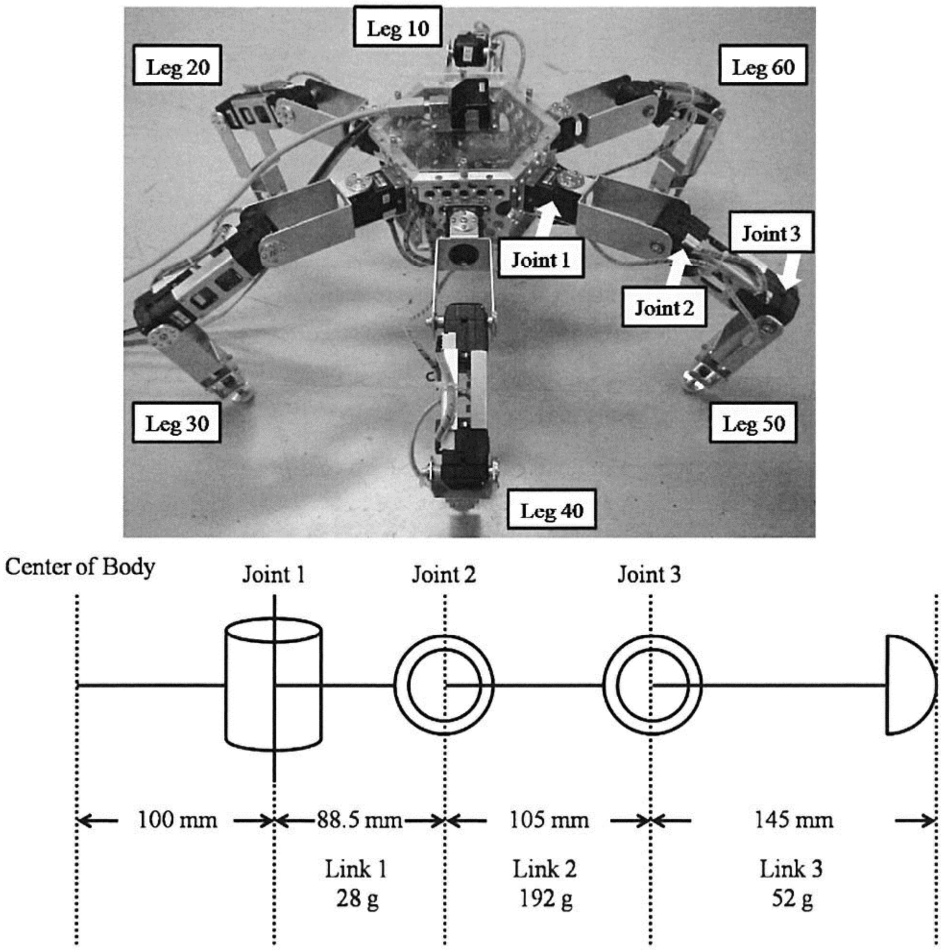

Figure 1. Limb mechanism robot ASTERISK and its leg configuration.

each joint from 1 to 3. The authors called each joint by a leg number and joint number, e.g., joint 21 means the first joint of leg number 20. The length and weight of each link is shown in Fig. 1. ASTERISK is made symmetric on both sides of its body, which allows the same workspace in the up and down directions. The robot's total weight is 2.67 kg, standard standing posture is 180 mm in height and 450 mm in width, and minimum standard walking gait width is about 210 mm.

From its features and maximum provided torque of 37 kg-cm, the authors chose the smart actuator module Dynamixel DX-117 by ROBOTIS for the joint actuators. This module contains a servo motor, a reduction gear, a control unit and a communication interface in a compact package. This module can generate enough motor torque to support the robots when using only three legs.

The authors would like to provide a robot that can fulfill human needs in work assistance or even human replacement; therefore, the main purpose is to provide the authors' own robot ASTERISK with high mobility, high work ability, and expanded application fields to tasks in dangerous and inaccessible environments for humans, into real-world practical applications. So far, this robot has realized many operations: omni-direction gait on flat and irregular terrain, walking on a grid ceiling, climbing up onto steps, continuous stair climbing with laser range scanning for stair recognition, climbing a ladder, passing through narrow tunnels, and manipulating objects using two neighboring limbs [6–8].

3. Rolling-Walk Strategy

Rolling-walk motion is a motion in which the robot walks in one direction while making a body rotation. This strategy was designed based on the omni-directional characteristic of ASTERISK. While the robot is walking with three legs, the robot should be able to walk through a narrow space that the normal walking gait cannot achieve, i.e., the space should be less than the minimum required space for the static gait (210 mm). Nevertheless, when the robot is standing up using three legs, its balance, joint torque and walking motion need to be carefully considered in order to perform a stable, safe walking motion.

In this research, the authors divided the gait into two phases for easier analysis of the rolling-walk gait: three-leg and two-leg supporting phases (Fig. 2). At the transition from the three-leg to two-leg supporting phase, the speed and acceleration of the robot's body has to achieve the minimum required value in order that the robot could maintain its stability. Furthermore, during the two-leg supporting phase, the area between two legs will become a single line and, therefore, it is difficult to control and keep the position of the zero moment point (ZMP) within that area. Those methods for controlling the motion will be discussed in later sections.

Before the robot can perform the dynamic rolling-walk motion, the robot has to vertically stand up first. The authors chose to design a standing-up motion in static to reduce complexities (Fig. 3). The processes of the standing-up motion are:

(i) Standard standing posture.

(ii) Legs arrangement: arrange legs into a suitable position for performing the standing-up motion.

(iii) 40° body y-rotation (five legs): after arranging the leg positions, the robot will rotate its body 40° in the y-direction.

(iv) Leg rearrangement: reduce the number of supporting legs from five to three legs.

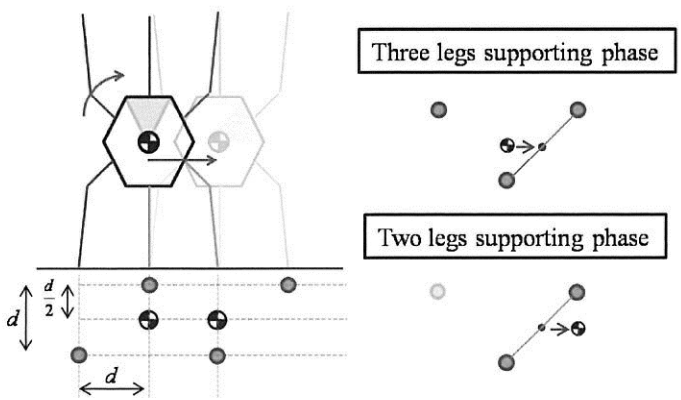

Figure 2. Rolling-walk motion.

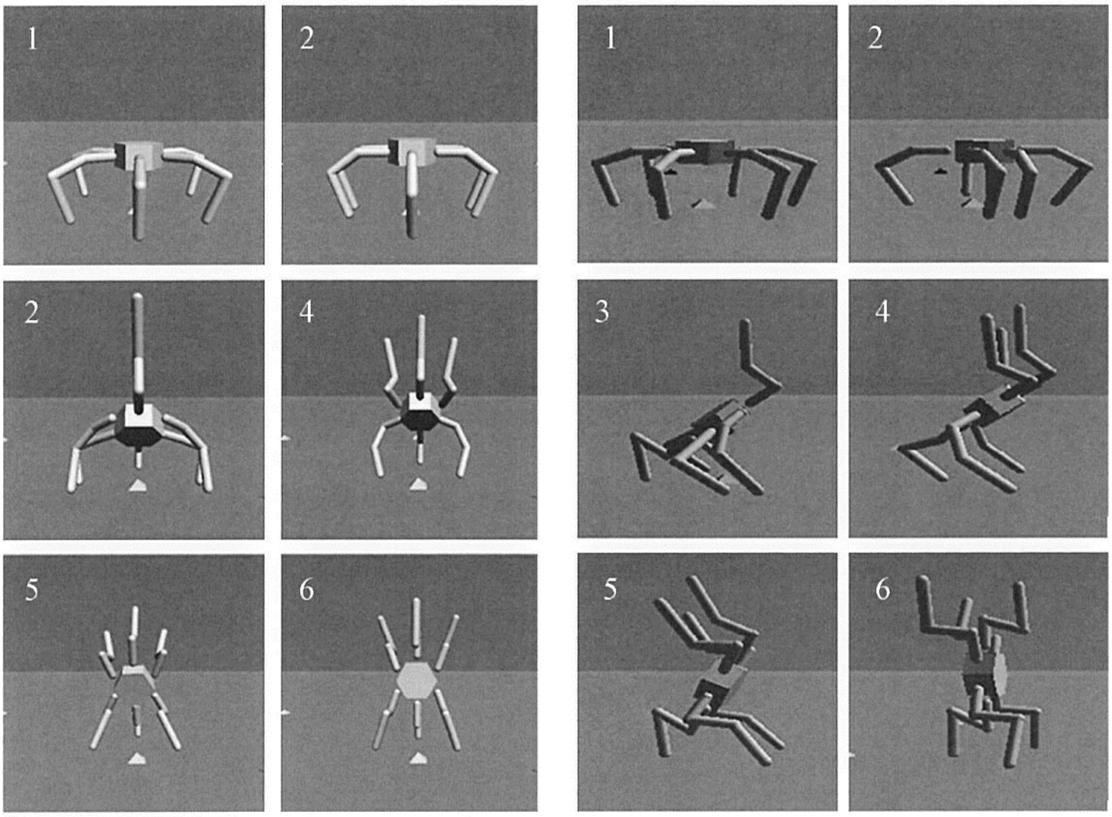

(a) (b)

Figure 3. Standing up motion (a) front view and (b) side view.

(v) Body rotation from 40° to 70°: after rearranging the leg positions, the robot will increase its height, change its leg orientation and rotate its body 70° in the x-direction.

(vi) Body rotation from 70° to 90°: at this stage, the robot will rearrange its upper legs to maintain its stability.

The experiment on the actual robot is shown in Fig. 4.

In this research, types of leg (Fig. 5), are defined as follows. Swing leg is a leg that will swing down from free legs to become one of the next supporting legs. The authors directly assigned the swing leg's speed so that it reaches the foot target position before it falls down. Next, supporting legs are the legs that keep contact with the ground during each phase. The authors control the motion of supporting legs by using preview control of the ZMP. Lastly, free legs are the legs that will be controlled by resolved momentum control and used to maintain the robot's balance at all times.

4. Preview Control of the ZMP

After the robot stands up, the preview control of the ZMP will be used to determine and generate the center of mass trajectory before the robot performs rolling-walk motion.

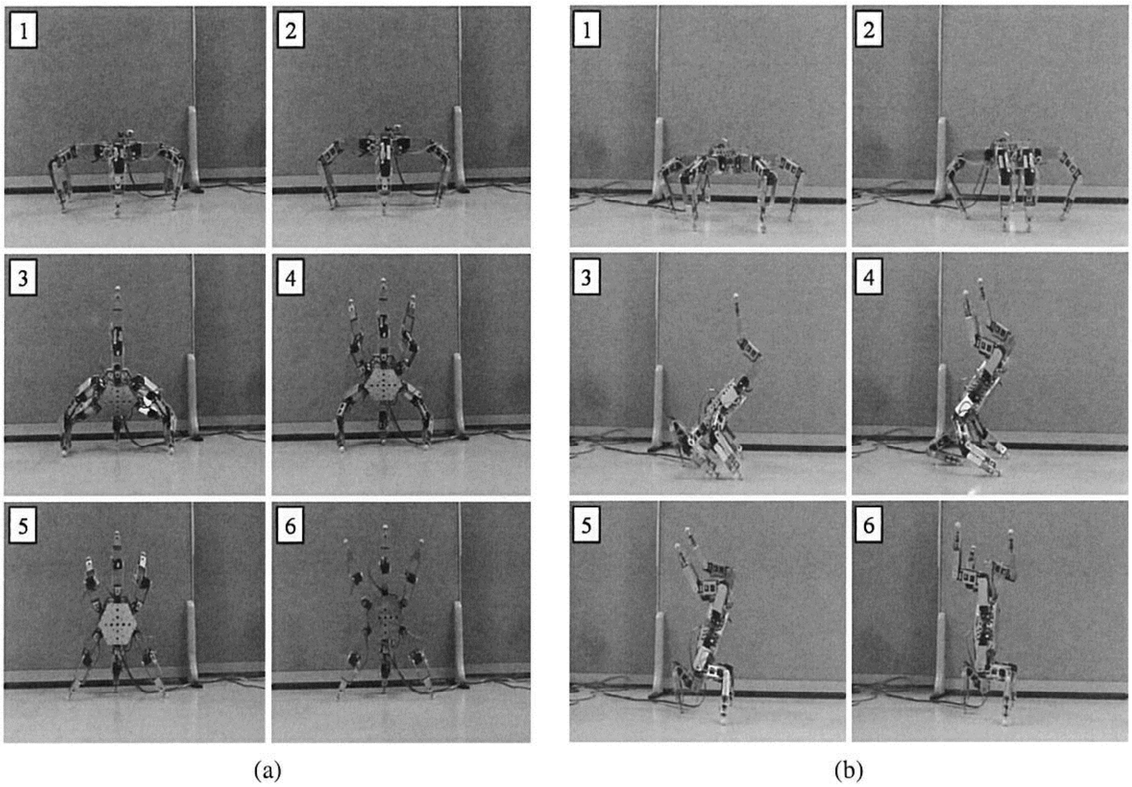

Figure 4. Standing up motion by actual robot (a) front view and (b) side view.

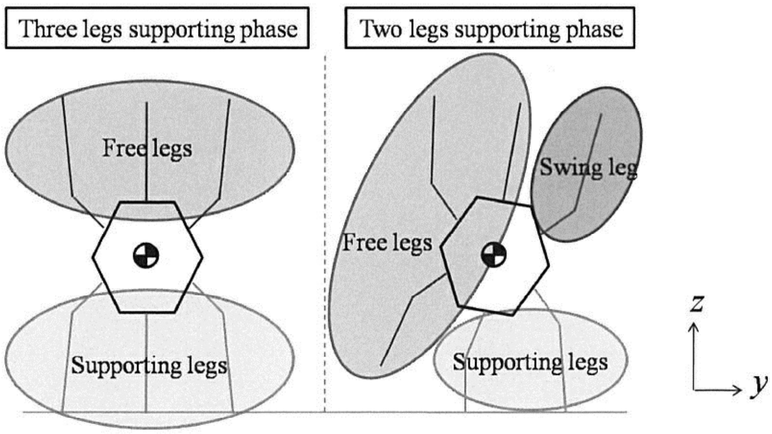

Figure 5. Types of legs.

The preview control of ZMP proposed by Kajita *et al.* [9] is a method to generate the center of mass trajectory to achieve a dynamic motion by using a cart-table model to represent a biped robot and giving the cart motion as the trajectory of the robot's center of mass.

4.1. ZMP Equation for the Cart-Table Model

Considering the cart-table model (Fig. 6), the ZMP equation can be derived by:

$$\tau_{\mathrm{ZMP}} = mg(y - p_y) - m\ddot{y}Z_c = 0. \quad (1)$$

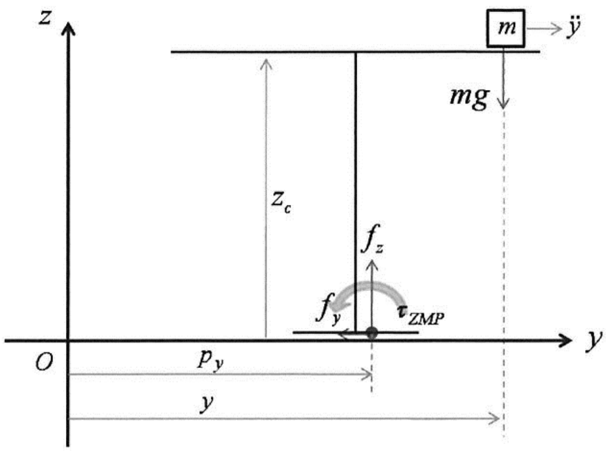

Figure 6. Cart-table model.

Then:

$$p_y = y - \frac{Z_c}{g}\ddot{y}, \tag{2}$$

where p_y is the distance from the origin to the ZMP, y is the distance from the origin to the cart's center of mass, Z_c is a height of center of mass and g is gravitational acceleration.

4.2. Pattern Generation by Preview Control

According to Ref. [9], the ZMP control system is discretized with input $u_y = \frac{d}{dt}\ddot{y}$ and sampling time T as:

$$\begin{aligned} y(k+1) &= Ay(k) + Bu(k) \\ p(k) &= Cy(k), \end{aligned} \tag{3}$$

where:

$$\begin{gathered} y(k) \equiv [\, y(kT) \quad \dot{y}(kT) \quad \ddot{y}(kT)\,]^{\mathrm{T}} \\ u(k) \equiv u_y(kT) \\ p(k) \equiv p_y(kT) \\ A \equiv \begin{bmatrix} 1 & T & T^2/2 \\ 0 & 1 & T \\ 0 & 0 & 1 \end{bmatrix} \\ B \equiv \begin{bmatrix} T^3/6 \\ T^2/2 \\ T \end{bmatrix} \\ C \equiv [\,1 \quad 0 \quad -Z_c/g\,]. \end{gathered}$$

Then, with the given ZMP reference, the performance index is specified as:

$$J = \sum_{i=k}^{\infty}\{Q_e e(i)^2 + \Delta y^{\mathrm{T}}(i) Q_y \Delta y(i) + R\Delta u^2(i)\}, \tag{4}$$

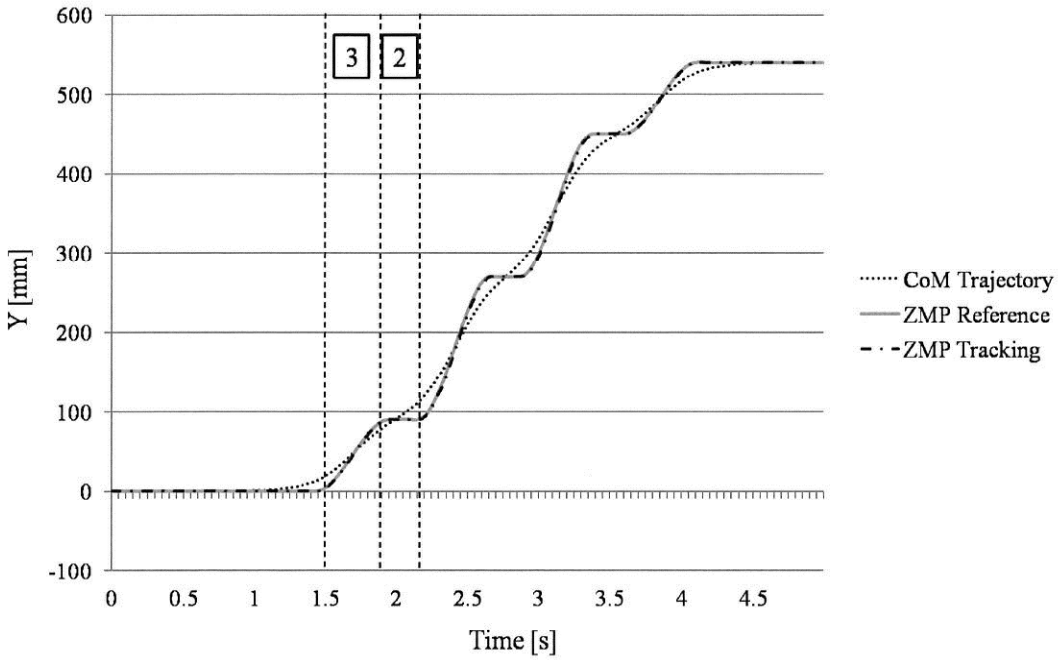

Figure 7. Result of preview control.

where $e(i) \equiv p(i) - p^{\mathrm{ref}}(i)$ is the servo error, Q_e, $R > 0$, and Q_y are a 3×3 symmetric non-negative definite matrix, $\Delta y(k) \equiv y(k) - y(k-1)$ is the incremental state vector, and $\Delta u(k) \equiv u(k) - u(k-1)$ is the incremental state input.

The optimal controller that minimizes the performance index when the previewed ZMP reference for the step future at every sampling time is given by:

$$u(k) = -G_i \sum_{i=0}^{k} e(k) - G_y y(k) - \sum_{j=1}^{N_L} G_p(j) p^{\mathrm{ref}}(k+j), \tag{5}$$

where N_L is the number of samples during the preview time, G_i, G_y and $G_p(j)$ are the gains calculated from the weight, Q_e, Q_y, R and the system parameter of (3). For more details, please refer to Ref. [9].

The result of the center of mass trajectory generated by the preview control with the previewing period of 1.42 s, two-leg supporting time of 0.21 s, three-leg supporting time of 0.51 s, sampling time of 30 ms, $Q_e = 1.0$, $Q_y = 0$ and $R = 1 \times 10^{-6}$ is shown in Fig. 7.

4.3. Torque Calculation Based on the Cart-Table Model

Normally, before any motion can be implemented in an actual robot, the required torque of each joints needs to be calculated and confirmed whether or not it exceeds the provided torque by an actuator. As the preview control of the ZMP generates the center of mass trajectory of the robot based on the cart-table model, the motion of the center of mass can be considered as one-dimensional motion that balances during each phase.

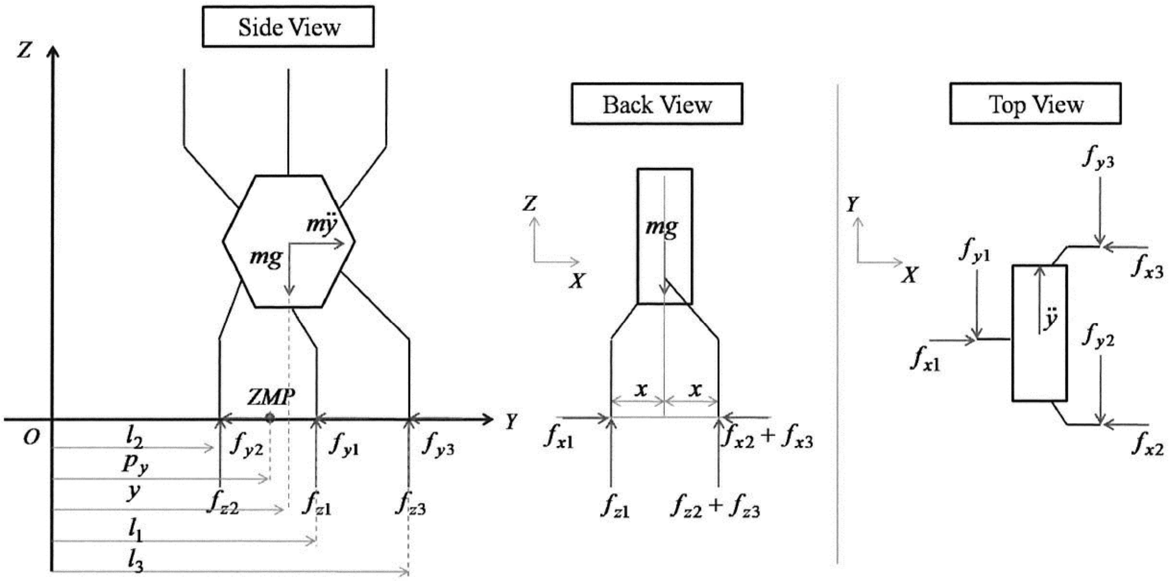

Figure 8. Torque calculation during three-leg supporting phase.

As the rolling-walk motion is a motion in the Y-direction only, during the three-leg supporting phase, forces in the X-, Y- and Z-axis for each leg can be calculated according to Fig. 8 as:

$$f_{x1} = f_{x2} = f_{x3} = 0 \tag{6}$$

$$f_{y1} = -\frac{m\ddot{y}}{2}, \qquad f_{y2} = f_{y3} = -\frac{m\ddot{y}}{4} \tag{7}$$

$$f_{z1} = \frac{mg}{2}, \qquad f_{z2} = \frac{mg}{2} - f_{z3}. \tag{8}$$

At the ZMP:

$$f_{z1}(l_1 - p_y) + f_{z2}(l_2 - p_y) + f_{z3}(l_3 - p_y) = 0. \tag{9}$$

Substitute (8) into (9) and simplify the equation, then:

$$f_{z2} = \frac{mg}{2}\left(\frac{l_3 + l_1 - 2p_y}{l_3 - l_2}\right) \quad \text{and} \quad f_{z3} = \frac{mg}{2}\left(\frac{2p_y - l_2 - l_1}{l_3 - l_2}\right). \tag{10}$$

Since the ZMP is fixed during the two-leg supporting phase (Fig. 7), the forces can be easily derived from Fig. 9 as:

$$f_{x1} = f_{x2} = 0 \tag{11}$$

$$f_{y1} = f_{y2} = -\frac{m\ddot{y}}{2} \tag{12}$$

$$f_{z1} = f_{z2} = \frac{mg}{2}. \tag{13}$$

After all forces are obtained in both phases, the required torque of each joint can be calculated by using the Jacobian matrix. The authors neglected the individual leg weight and instead used the whole robot weight of 2637 g in the calculation.

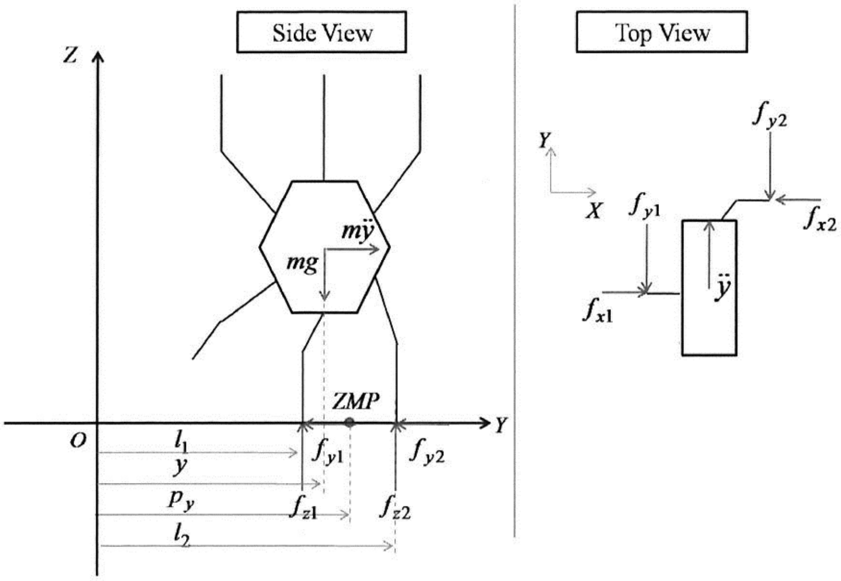

Figure 9. Torque calculation during two-leg supporting phase.

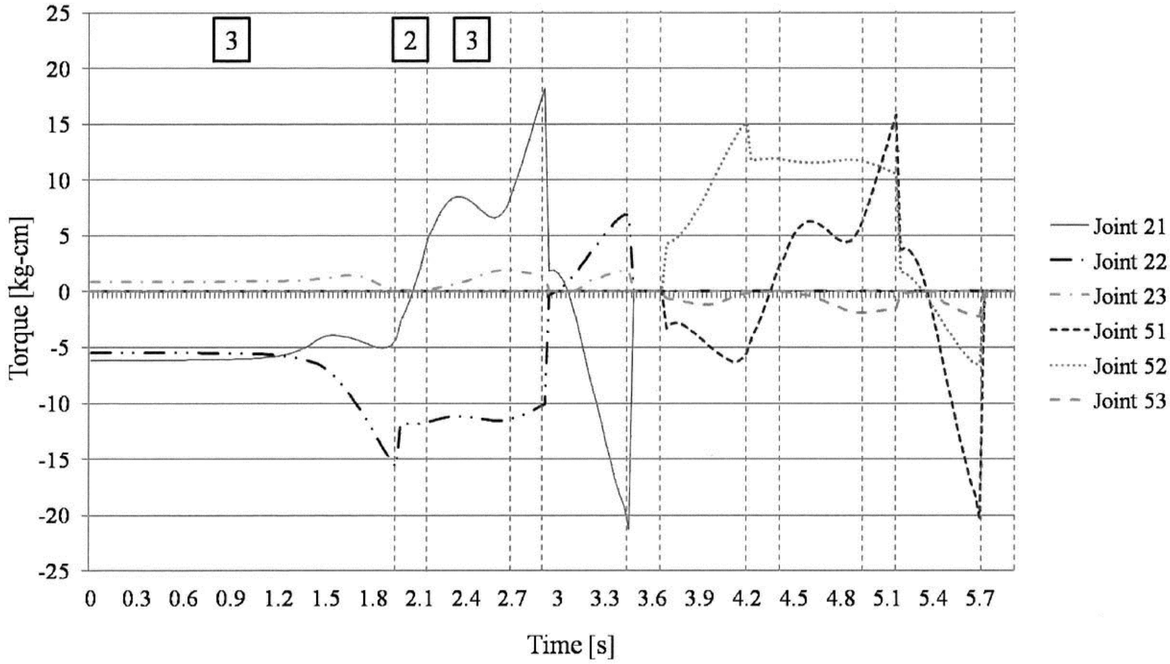

Figure 10. Example of torque required for supporting legs during the motion (leg 20 and 50).

An example of the required torque for supporting legs during six cycles of rolling-walk motion (360° of rotation, 1080 mm of center of mass trajectory in the Y-direction) is shown in Fig. 10. It shows that the maximum required torque is within the torque provided by an actuator. As this motion is a periodic motion, it also shows that the torque required for each leg 20's joint is similar to leg 50's and the only difference is the torque direction in joint 2 and 3.

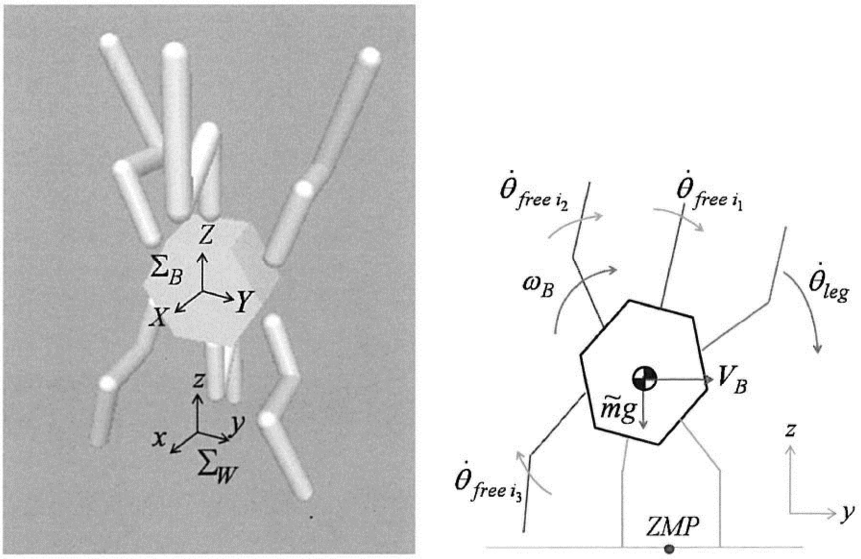

(a) (b)

Figure 11. (a) Model of ASTERISK and (b) resolved momentum control during two-leg phase.

5. Resolved Momentum Control

Resolved momentum control is a method to generate a whole-body motion of a robot such that the resulting total linear and angular momenta become specified values. Kajita *et al.* [10] introduced this method for a humanoid robot. They suggested and demonstrated that no matter how complicated a structure, a robot has, its total linear and angular momenta can still be determined. Since the momentum vector and joint speed vector have a linear relationship, a humanoid's balancing, walking and other motions can be easily generated by this method.

In the case of ASTERISK, the resolved momentum control will be used only to control the robot's free legs to balance itself during the rolling-walk motion (Fig. 11). The authors simplified the relationship between the total linear and angular momenta of the robot and body velocity and angular velocities, swing leg's joint speed $\dot{\theta}_{\mathrm{leg}}$ and free legs' joint speed $\dot{\theta}_{\mathrm{free}}$ in the world coordinate Σ_{W} as:

$$\begin{bmatrix} P \\ L \end{bmatrix} = \begin{bmatrix} \tilde{m}E & 0 \\ 0 & \tilde{I} \end{bmatrix} \begin{pmatrix} V_{\mathrm{B}} \\ \omega_{\mathrm{B}} \end{pmatrix} + \begin{bmatrix} M_{\mathrm{leg}} \\ H_{\mathrm{leg}} \end{bmatrix} \dot{\theta}_{\mathrm{leg}} + \begin{bmatrix} M_{\mathrm{free}} \\ H_{\mathrm{free}} \end{bmatrix} \dot{\theta}_{\mathrm{free}}, \qquad (14)$$

where P and L are whole-body linear and angular momenta, $\tilde{m}$ is the robot mass, $\tilde{I}$ is the 3×3 inertia matrix with respect to the center of mass, V_{B} and ω_{B} are the body linear and angular velocities, and M and H are the $3 \times n$ inertia matrices that indicate how the joint speeds affect the linear and angular momenta of the robot where n is the total number of joints. For more information on M and H calculation, refer to Ref. [10]. Note that, in this calculation, the weights of all individual parts will be taken in to account.

As the goal of resolved momentum control of this experiment for ASTERISK is to calculate the free legs' joint speed that would generate the whole-robot desired linear and angular momenta, the body linear velocity could be obtained from the preview control of the ZMP, and the swing leg's joint speed and the body angular velocity were directly assigned by the authors, the free legs' joint speed can be calculated from (14) as:

$$\dot{\theta}_{\text{free}} = A^{t}\left[\begin{bmatrix} P^{\text{ref}} \\ L^{\text{ref}} \end{bmatrix} - \begin{bmatrix} \tilde{m}E & 0 \\ 0 & \tilde{I} \end{bmatrix}\begin{bmatrix} V_{\text{B}} \\ \omega_{\text{B}} \end{bmatrix} - \begin{bmatrix} M_{\text{leg}} \\ H_{\text{leg}} \end{bmatrix}\dot{\theta}_{\text{leg}}\right], \tag{15}$$

where A^{t} is a pseudo-inverse of $\begin{bmatrix} M_{\text{free}} \\ H_{\text{free}} \end{bmatrix}$.

Due to the facts that the robot moves only in the Y-direction and rotates only the around the $-X$-axis, the target momentum was given such that the robot could maintain its balance as:

$$P_{y}^{\text{ref}} = \tilde{m}(\tilde{c}_{y}^{\text{ref}} - \tilde{c}_{y}), \qquad P_{x,z}^{\text{ref}} = 0$$

$$L_{x}^{\text{ref}} = -\tilde{I}\left(\frac{\Delta\theta_{\text{B},x}}{T_{\text{p}}}\right), \qquad L_{y,z}^{\text{ref}} = 0,$$

where $\tilde{c}_{y}^{\text{ref}}$ is the target center of mass position obtained from the preview control of the ZMP, $\tilde{c}_{y}$ is the current center of mass position, $\Delta\theta_{\text{B},x}$ is the change of body angle and T_{p} is the sampling period.

6. Implementation of Error Compensation

After the motion was implemented and tested with an actual robot, the authors found that there are errors from the actuator that make the robot unstable and that cause the robot's body to shake until the end of the motion or even fall down (Fig. 12). Therefore, the authors decided to go with error compensation.

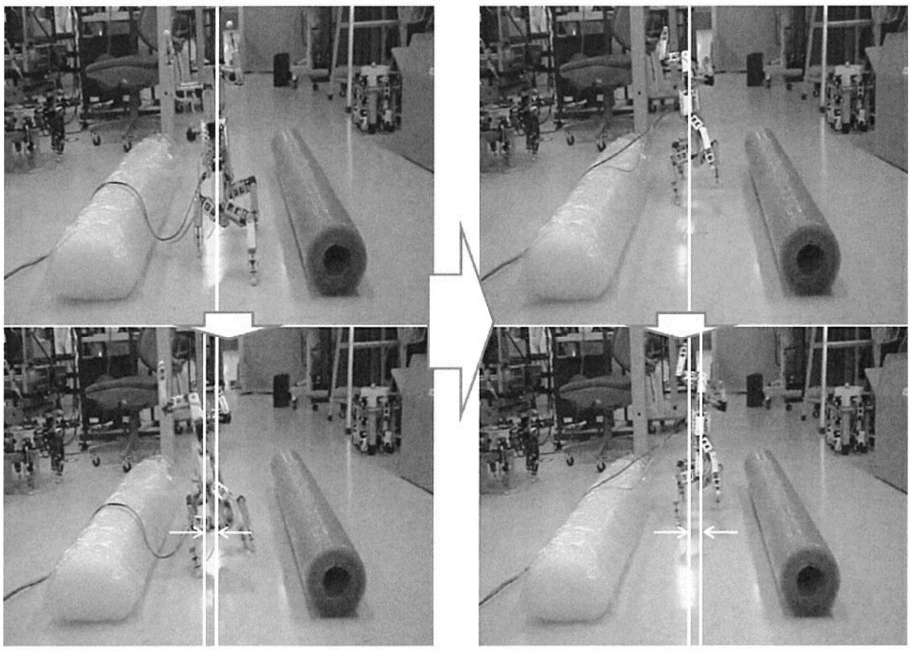

Figure 12. Robot's body tilted.

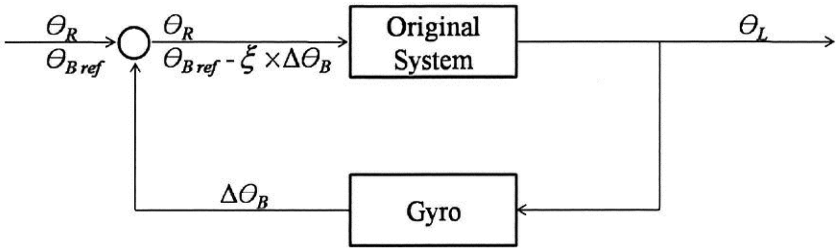

Figure 13. Error compensation system.

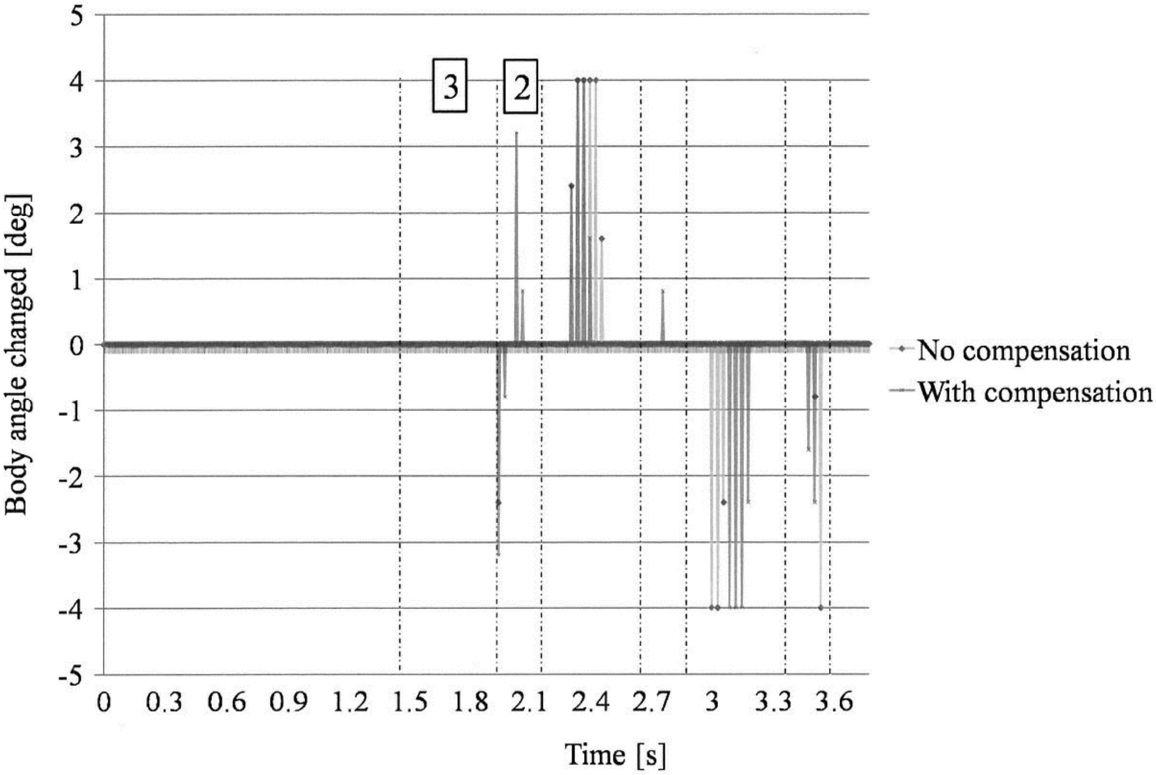

Figure 14. Data from gyro.

The authors chose the MDP-A3U9 sensor from NEC/TOKIN and used its gyro sensor to compensate for errors by adjusting the Y-body angle in the world coordinate based on the assumption that during the three-leg supporting phase the robot will always be in balance and, therefore, no error compensation will be applied. The diagram of the gyro sensor implementation is shown in Fig. 13. The Y-body rotation of robot can be calculated by:

$$\theta_{\mathrm{B}} = \theta_{\mathrm{Bref}} - \xi \times \Delta\theta_{\mathrm{B}}, \tag{16}$$

where θ_{B} is the Y-body angle in the world coordinate, θ_{Bref} is the Y-body ideal angle in the world coordinate and equal to $-90°$, θ_{R} is the body rotation according to the rolling-walk motion, θ_{L} is the actuator target angle, $\Delta\theta_{\mathrm{B}}$ is the Y-body angle changed reading from the gyro sensor and ξ is the gain to compensate the error.

Data from the gyro sensor was taken to compare the effect of the error compensation (Fig. 14). The error from the first step led to the body vibration towards the

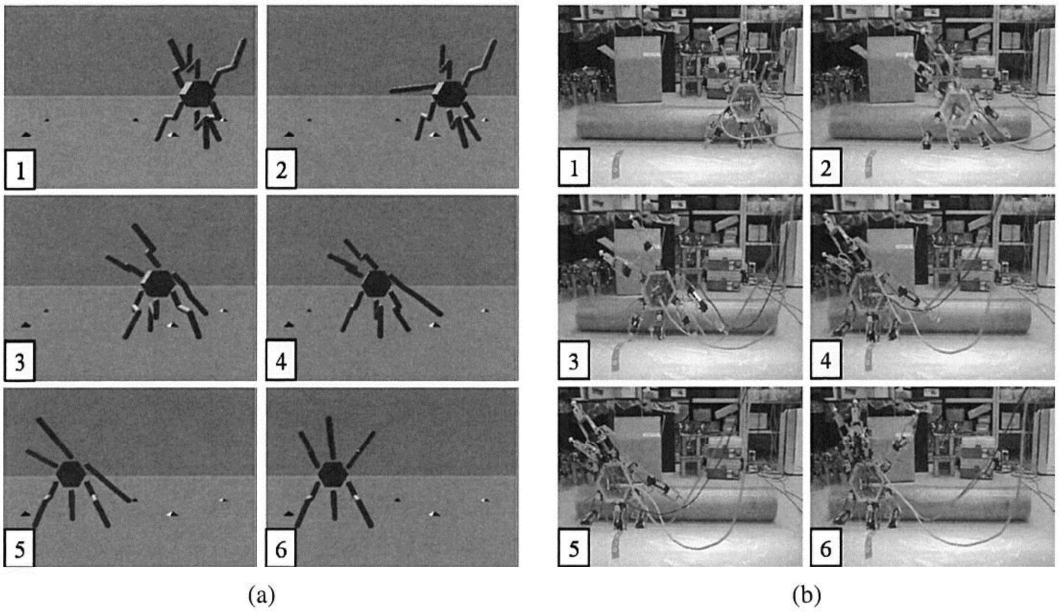

Figure 15. Result of dynamic rolling-walk motion (a) in ODE and (b) with error compensation.

end of the motion. The motion with error compensation has less body vibration as compared to the motion without compensation.

7. Results

The three cycles of new dynamic rolling-walk motion were confirmed by using Open Dynamics Engine (ODE) [13] as a dynamics simulator and an actual robot (Fig. 15). The authors chose parameter d in Fig. 2 as 180 mm with a body height of 280 mm in this experiment. After the first experiment failed, the authors implemented the error compensation system. For the second experiment after the error compensation was implemented, the motion was improved. The results of actual robot rolling-walk motion with and without error compensation are compared and shown in Fig. 16. Figure 16 shows the comparison of the robot's body vibration after the motion stopped. The motion with error compensation could reduce the vibration angle from 6.14° to 2.58° (which is about 58%).

8. Conclusion

The authors designed a new dynamic rolling-walk motion for a mobile robot so that it can walk through narrow spaces where static motion cannot be achieved. In addition, they also developed and applied the preview control of the ZMP and resolved momentum control of a biped robot to the limb mechanism robot ASTERISK as dynamic rolling-walk motion controllers. The motion was confirmed in ODE as a dynamics simulator before being implemented in an actual robot. After the first experiment with the actual robot, the authors found a problem in that the robot's body tilted after the first step and they decided to implement the error compensation sys-

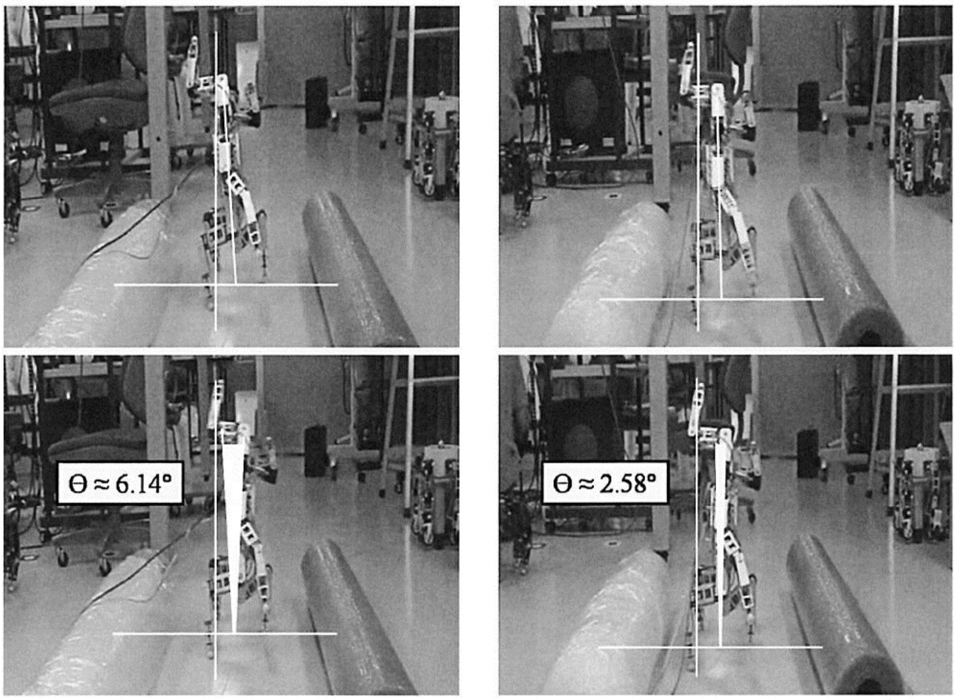

(a) (b)

Figure 16. Vibration at the end of (a) motion without and (b) motion with error compensation.

tem. Finally, the dynamic rolling-walk motion was achieved in both the simulator and actual robot.

Due to the physical limitations of the robot, the authors could not explore a range of walking speeds, step lengths, body heights, and other parameters. For future work, the authors plan to explore those parameters to see how their variation will affect the motion. Additionally, to further improve the mobility of the rolling-walk motion and make it more practical, the authors also plan to design a turning motion for rolling-walk motion.

Acknowledgements

This work was partially supported by the Ministry of Education, Science, Sports and Culture, Grant-in-Aid for Scientific Research (B), 18360123, 2009.

References

1. I. Morazzani, D. Lahr, D. Hong and P. Ren, Novel tripedal mobile robot and considerations for gait planning strategies based on kinematics, in: *Proc. IEEE Int. Conf. on Robotics and Automation*, Rome, pp. 2776–2777 (2007).
2. R. T. Schroer, M. J. Boggess, R. J. Bachmann, R. D. Quinn and R. E. Ritzmann, Comparing cockroach and whegs robot body motions, in: *Proc. IEEE Conf. on Robotics and Automation*, New Orleans, LA, vol. 4, pp. 3288–3293 (2004).
3. E. Z. Moore, D. Campbell, F. Grimminger and M. Buehler, Reliable stair climbing in the simple hexapod RHex, in: *Proc. IEEE Int. Conf. on Robotics and Automation*, Washington, DC, pp. 2222–2227 (2002).

4. T. McGeer, Passive dynamic walking, *Int. J. Robotics Res.* **9**, 62–82 (1990).
5. J. Sastra, S. Chitta and M. Yim, Dynamic rolling for a modular loop robot, *Int. J. Robotics Res.* **28**, 758–773 (2009).
6. C. Theeravithayangkura, T. Takubo, Y. Mae and T. Arai, Stair recognition with laser range scanning by limb mechanism robot ASTERISK, in: *Proc. IEEE Int. Conf. on Robotics and Biomimetics*, Bangkok, pp. 915–920 (2009).
7. T. Takubo, T. Arai, K. Inoue, H. Ochi, T. Konishi, T. Tsurutani, Y. Hayashibara and E. Koyanagi, Integrated limb mechanism robot ASTERISK, *J. Robotics Mechatron.* **18**, 203–214 (2006).
8. S. Fujii, K. Inoue, T. Takubo and T. Arai, Climbing up onto steps for limb mechanism robot ASTERISK, in: *Proc. 23rd Int. Symp. on Automation and Robotics in Construction*, Tokyo, pp. 225–230 (2005).
9. S. Kajita, F. Kanehiro, K. Kaneko, K. Fujiwara, K. Harada, K. Yokoi and H. Hirukawa, Biped walking pattern generation by using preview control of zero-moment point, in: *Proc. IEEE Int. Conf. on Robotics & Automation*, Taipei, pp. 1620–1626 (2003).
10. S. Kajita, F. Kanehiro, K. Kaneko, K. Fujiwara, K. Harada, K. Yokoi and H. Hirukawa, Resolved momentum control: humanoid motion planning based on the linear and angular momentum, in: *Proc. IEEE/RSJ Int. Conf. on Intelligent Robots and Systems*, Las Vegas, NV, pp. 1644–1650 (2003).
11. C. Theeravithayangkura, T. Takubo, K. Ohara, Y. Mae and T. Arai, Dynamic rolling-walk motion by limb mechanism robot ASTERISK, in: *Proc. IEEE Int. Conf. on Mechatronics and Automation*, Changchun, pp. 2659–2664 (2009).
12. C. Theeravithayangkura, T. Takubo, K. Ohara, Y. Mae and T. Arai, Dynamic rolling-walk motion with sensory compensation, in: *Proc. IEEE Int. Conf. on Robotics and Biomimetics*, Guilin, pp. 592–597 (2009).
13. R. Smith, Open dynamics engine, available at www.ode.org
14. O. Matsumoto, S. Kajita and K. Tani, Estimation and control of the attitude of a dynamic mobile robot using internal sensors, *Adv. Robotics* **7**, 159–178 (1993).
15. S. Hirose, K. Yoneda, K. Arai and T. Ibe, Design of a quodruped walking vehicle for dynamic walking and stair climbing, *Adv. Robotics* **9**, 107–124 (1995).
16. J.-H. Kim and J.-H. Oh, Realization of dynamic walking for the humanoid robot platform KHR-1, **18**, 749–768 (2004).
17. J.-Y. Kim, I.-W. Park and J.-H. Oh, Experiment realization of dynamic walking of the biped humanoid robot KHR-2 using zero moment point feedback and inertial measurement, *Adv. Robotics* **20**, 707–736 (2006).

About the Authors

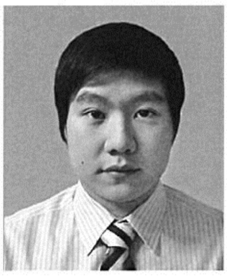

Chayooth Theeravithayangkura obtained his BE degree in the Electrical Engineering field from Sirindhorn International Institute of Technology, Thammasat University, Prathumtani, Thailand, in 2004, and MS degree from Osaka University, Osaka, Japan, in 2009, where he is currently working toward his PhD degree in Systems Science and Applied Informatics. His research interests include dynamic motions, mobile robots and multi-legged robots. He is a Student Member of the Robotic Society of Japan.

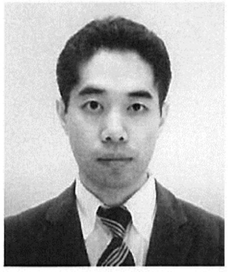

Tomohito Takubo received the MS and PhD degrees, all in Mechanical Engineering, from Tsukuba University, Japan, in 2000 and 2003, respectively. He has been an Assistant Professor in the Department of Systems Innovation, Graduate School of Engineering Science, Osaka University, Japan, since 2007. He was a Research Associate at Osaka University, Japan, from 2004. He was a Postdoctoral Fellow at Osaka University, Japan, from 2003. His major research interests are humanoid robots, human–robot cooperation, multi-leg robots and multi-scale manipulation.

Kenichi Ohara received the MS degree in Electrical Engineering from Shibaura Institute of Technology, Tokyo, Japan, in 2004, and PhD degree from the University of Tsukuba, Tsukuba, Japan, in 2008. Since April 2007, he has been a Member of the Ubiquitous Function Research Group, Intelligent Systems Research Institute, National Institute of Advanced Industrial Science and Technology, Tsukuba, and since May 2007, he has been an Assistant Professor with the Interfaculty Initiative in Information Studies, Graduate School of Interdisciplinary Information Studies, University of Tokyo, Tokyo. Since April 2008, he has been an Assistant Professor with the Department of Systems Innovation, Graduate School of Engineering Science, Osaka University, Osaka, Japan. His research interests include robot vision, wireless sensor networks and middleware technology for robots. He is a Member of the Robotics Society of Japan and the Japan Society of Mechanical Engineers.

Yasushi Mae received the BS, MS and PhD degrees in Engineering from Osaka University, Osaka, Japan in 1993, 1995 and 1998, respectively. From 1998 to 2004, he was a Research Associate in the Graduate School of Engineering Science, Osaka University. From 2004 to 2007, he was an Associate Professor in the Faculty of Engineering, University of Fukui. He moved to Osaka University, in 2007. He is currently an Associate Professor in the Department of Systems Innovation, Graduate School of Engineering Science, Osaka University, Osaka, Japan. His research interests include robot vision, working mobile robots and intelligent environments. He is a member of the IEEE, Robotics Society of Japan, Japan Society of Mechanical Engineers, Institute of Electronics, Information and Communication Engineers, Information Processing Society of Japan, and Virtual Reality Society of Japan.

Tatsuo Arai received the BS, MS and PhD degrees from the University of Tokyo in 1975, 1977 and 1986, respectively. He joined the Mechanical Engineering Laboratory, AIST, MITI (now METI), in 1977, and was engaged in research and development of new arm design and control, mobile robot, teleoperation, and micro robotics. He stayed at MIT as a Visiting Scientist, during 1986–1987. He moved to Osaka University, in 1997, and since then he has been a Full Professor in the Department of Systems Innovation, Graduate School of Engineering Science. His current research topics are mechanism design including parallel mechanisms, legged working robots, micro robotics for bio applications, humanoid robots and haptic interfaces. He is a Member of IEEE, the International Association of Automation and Robotics in Construction, and the Robotic Society of Japan.